(2)

Technical Report

Effect of Adsorbed Arsenic on the Decomposition Rate of Nickel Hydride

A. Kimura and H. K. Birnbaum
Department of Materials Science and Engineering
University of Illinois
1304 W. Green Street
Urbana, IL 61801

August 1989

USN 00014-83-K-0468
Office of Naval Research

REPORT DOCUMENTATION PAGE

READ INSTRUCTIONS BEFORE COMPLETING FORM

1. REPORT NUMBER

2. GOVT ACCESSION NO.

3. RECIPIENT'S CATALOG NUMBER

4. TITLE (and Subtitle)
Effect of Adsorbed Arsenic on the Decomposition Rate of Nickel Hydride

5. TYPE OF REPORT & PERIOD COVERED
Technical 8/89

6. PERFORMING ORG. REPORT NUMBER

7. AUTHOR(s)
A. Kimura and H.K. Birnbaum

8. CONTRACT OR GRANT NUMBER(s)
USN 00014-83-K-0468

9. PERFORMING ORGANIZATION NAME AND ADDRESS
University of Illinois
Department of Materials Science & Engineering
Urbana, IL 61801

10. PROGRAM ELEMENT, PROJECT, TASK AREA & WORK UNIT NUMBERS

11. CONTROLLING OFFICE NAME AND ADDRESS
Office of Naval Research
100 N. Quincy Ave.
Arlington, VA

12. REPORT DATE
August 1989

13. NUMBER OF PAGES
28

14. MONITORING AGENCY NAME & ADDRESS(if different from Controlling Office)

15. SECURITY CLASS. (of this report)
Unclassified

15a. DECLASSIFICATION/DOWNGRADING SCHEDULE

16. DISTRIBUTION STATEMENT (of this Report)
This report is unclassified. Reproduction and distribution for any purpose of the U.S. government is permitted.

17. DISTRIBUTION STATEMENT (of the abstract entered in Block 20, if different from Report)

18. SUPPLEMENTARY NOTES

19. KEY WORDS (Continue on reverse side if necessary and identify by block number)
Hydrogen
Hydrides
Cathodic charging
Electrolysis

20. ABSTRACT (Continue on reverse side if necessary and identify by block number)

The decomposition rate of nickel hydride was studied using x-ray, Auger spectroscopy, and SIMS techniques. In high purity nickel, which was cathodically charged with hydrogen, deposition of arsenic on the nickel surface considerably decreased the decomposition rate of nickel hydride. This effect of arsenic on the egress of hydrogen from nickel is related to the influence of adsorbed arsenic on the entry of hydrogen into nickel during cathodic charging. Both effects result from inhibition of the recombination

of hydrogen atoms at the surface thus resulting in a higher effective hydrogen fugacity at the surface. The effects of adsorbed arsenic on the decomposition of nickel hydride was influenced by alloying elements such as carbon and sulfur in the nickel, with the arsenic effect being greater in Ni-S alloys and smaller in Ni-C alloys than in high purity nickel.

Effect of Adsorbed Arsenic on the Decomposition Rate of Nickel Hydride

A. Kimura and H.K. Birnbaum
Department of Materials Science
University of Illinois at Urbana-Champaign
Urbana, IL 61801

Abstract

The decomposition rate of nickel hydride was studied using x-ray, Auger spectroscopy, and SIMS techniques. In high purity nickel, which was cathodically charged with hydrogen, deposition of arsenic on the nickel surface considerably decreased the decomposition rate of nickel hydride. This effect of arsenic on the egress of hydrogen from nickel is related to the influence of adsorbed arsenic on the entry of hydrogen into nickel during cathodic charging. Both effects result from inhibition of the recombination of hydrogen atoms at the surface thus resulting in a higher effective hydrogen fugacity at the surface. The effects of adsorbed arsenic on the decomposition of nickel hydride was influenced by alloying elements such as carbon and sulfur in the nickel, with the arsenic effect being greater in Ni-S alloys and smaller in Ni-C alloys than in high purity nickel.

MRL-89-015
8/22/89

I. INTRODUCTION

Electrolytic cathodic charging has often been used to introduce hydrogen into metals because of its convenience and the high hydrogen fugacities is developed on metal surfaces. It is well known that the addition of a small amount of "poison" such as As, CN^-, S^{2-} etc. in the electrolytic solution promotes hydrogen ingress into metals (1). The effect of As in the electrolyte on this process has been extensively investigated with particular attention to the chemical form of the arsenic compound. The most effective form of arsenic has been variously reported AsO_2^-(2), AsH_3(3,4) and elemental As (5,6). McBreen et al. (2) have reported that the increased rate of hydrogen entry is caused by a decrease of the hydrogen chemisorption energy due to anions such as AsO_2^-. Newman et al (3) found that the amount of hydrogen adsorbed on the surface is related to the bond strength of arsine (AsH_3) and that As is effective in increasing the H fugacity only in the range of pH in which the arsine is stable. In contrast to this view McCright et al (5) claimed that elemental As rather than arsine (AsH_3) is the dominant species in the hydrogen promotion mechanism. A recent result by Hagi et al (6) suggested that a layer of elemental arsenic deposited on the iron surface made hydrogen ingress easier than without the arsenic layer. It is clear that while the addition of As into the electrolyte increases the hydrogen surface fugacity the mechanism by which this occurs is still unclear.

The effect of As and other adsorbed species on hydrogen loss from metals has not been extensively studied. Smialowski (7) reported briefly that the outgassing rate from a hydrogen charged steel was decreased by As deposition on the surface. J. Pielaszek (8) found that the rate of decomposition of nickel hydride depended on the amount of prestraining before hydrogen charging and He concluded that dislocations stabilized the

hydride. He also observed that the nickel hydride stability was decreased by the addition of about 10^{-5} M Cu^{2+} ions to the electrolyte and postulated that this decreased stability was due to selective deposition of copper on the dislocations.

In the present work, the decomposition rate of nickel hydride was measured by x-ray and SIMS techniques after cathodic charging and as a function of the surface chemistry of the specimen. The decomposition rate was measured for hydride formation in high purity nickel, nickel carbon alloys and nickel sulfur alloys. The kinetics of hydrogen ingress and egress and the effects of arsenic will be discussed in the light of these experimental results.

II. EXPERIMENTAL METHODS

High purity (99.999%) nickel sheet (1.5 mm thickness) was annealed at 1173 K for 3 days in 1 atm of purified hydrogen gas to remove interstitial impurities. These specimens are denoted HP-Ni. Carburization of the HP-Ni was carried out by annealing in 90% CO/10% CO_2 at 1223 K for 24 h followed by quenching into oil. Sulfur was introduced into the HP-Ni by annealing in H_2S-H_2 (1 ppm H_2S) mixtures at 1173 K for 4 days. Sulfur doped specimens were then annealed briefly n H_2 gas at 1173 K and quenched to uniformly distribute the S. These specimens were then cold rolled to a thickness of 0.8 mm and recrystallized in vacuum (4×10^{-4} Pa) at 773 K for 1 hr. Chemical analysis of the three types of specimens are shown in Table 1. The average grain diameter of these three types of specimens were all determined to be about 15 μm.

Specimens were electro-polished in a sulfuric acid solution (H_2SO_4 : H_2O = 3 : 2) then electrolytically charged with H(D), in an electrolyte of (IN) 1 N

H_2SO_4 (D_2SO_4 for the SIMS study) to which 10 mg/l of $NaAsO_2$ was added as a "poison" or in the electrolyte with no added "poison." The specimen was the cathode, and a a platinum anode was used at a current density of 500 A/m^2. Charging generally proceeded for 20 min. at 293 K except where otherwise specified. After charging, the specimen was washed briefly with water and rinsed with methanol and acetone within 1 min of removal from the electrolyte.

X-ray diffraction experiments were performed to measure the thickness of nickel hydride using Cu K_α radiation at 35 kV and 15 mA. The peak height of the {111} nickel hydride peak was measured at 298 K during aging in air at 298 K while the specimen remained mounted on the diffractometer. Secondary Ion Mass Spectroscopy (SIMS) measurements were carried out to measure the thickness of nickel deuteride and its decomposition rate. These measurements were performed in a Cameca SIMS using a C_s^+ ion source. The nickel specimens used for SIMS measurements were cathodically charged with deuterium (^2H) using D_2SO_4 ($^2H_2SO_4$) to maximize the signal to noise ratio during the SIMS measurement (9). The depth profiling of several atomic masses were carried out with a 500 x 500 μm sputtered area and 60 x 60 μm analyzed area at a specimen temperature below 200 K. The sputtering rate was determined by measuring the depth of the sputtered pit after the SIMS measurement. Since the SIMS method is not suitable for determination of surface adsorbed species, a measurement of arsenic deposition on the nickel surface was investigated by Auger Electron Spectroscopy (AES).

III. EXPERIMENTAL RESULTS

1. Decomposition of Nickel Hydride

The typical features of the x-ray diffraction peaks of HP-Ni which was hydrogen charged in the presence of $NaAsO_2$ (Fig. 1 (b)) and aged (Fig. 1(c)) are compared with those of HP-Ni before charging (Fig. 1(a)). Hydrogen charging in an electrolyte containing $NaAsO_2$ caused the appearance of extra reflections which were evaluated to be from nickel hydride; which has an fcc lattice structure and a lattice parameter of 3.7263A (10,11). tFor the twenty minute charging times used these hydride peaks were observed only when arsenic was added in an electrolytic solution; in the absence of $NaAsO_2$ no hydride reflections were observed even for cathodic current densities as high as 1000 A/m^2. The presence of these hydride reflections is not specific to the use of $NaAsO_2$ in the electrolyte as these extra peaks have been observed for nickel charged in an electrolytic solution which contained thiouria instead of arsenic (10).

After aging in air at 298 K for 43 h (Fig. 1(c)), the peak heights of the nickel hydride reflections decreased, while those of nickel increased as expected from the decomposition of nickel hydride near the surface. It is noteworthy that it requires a much longer time to decompose the hydride (43 h) than to form it (20 min). Figure 2 shows the dependence of the decomposition rate and peak height of the {111}* nickel hydride peak, $I_{\{111\}^*}$ on the charging current density and charging time. The amount of surface hydride formed, as measured by $I_{\{111\}^*}$, increases with charging time and with the cathodic current density. The hydride decomposition rate (Fig. 2) on aging in air at 298 K was initially very low. The initial aging period, during which the $I_{\{111\}^*}$ remained essentially constant, increased as the hydride thickness increased. As will be discussed subsequently, the hydride thickness for these charging conditions was about 1 micrometer. Since the absorption thickness for Cu K_α in NiH is 24.5 micrometers, this constancy of $I_{\{111\}^*}$ was not caused

by limited x-ray penetration but reflected the actual constancy of the hydride thickness. Subsequent to this initial aging period the amount of hydride on the surface decreased with the rate of decrease $dI_{\{111\}^*}/dt$ being largest for conditions where the smallest amount of hydride was initially formed.

This somewhat unusual aging behavior is consistent with the phase diagram of the Ni-H system which has a miscibility gap between the solid solution α and the β hydride (10,11). The variation of the intensity of the $\{111\}^*$ reflection suggests that the initial loss of hydrogen on aging did not affect the amount of β hydride. Changes in the crystallographic parameters which accompany hydride decomposition at 298 K are shown in Fig. 3. In this data, as well as for that shown in Fig. 2, $I_{\{111\}^*}$ increased slightly after about 50 min aging, and then began to decrease after about 100 min. This small initial increase of $I_{\{111\}^*}$ was always observed during the first aging of hydrogen charged nickel. After outgassing subsequent cathodic charging and aging did not exhibit this initial increase in the hydride peak intensities. The intensities of the Ni reflections began to increase at the time that $I_{\{111\}^*}$ began to decrease; consistent with conversion of the β hydride to the α solid solution. The 2θ values of the nickel hydride β phase gradually increased during the initial aging period while the 2θ values of the α solid solution remained constant. As the $I_{\{111\}^*}$ decreased and $I_{\{111\}}$ increased the α and β lattice parameters (2θ values) remained constant.

These changes in the x-ray intensities and lattice parameters are consistent with the aging behavior of a cathodically formed exterior β hydride are consistent with the expected aging behavior of a cathodically formed exterior β hydride in equilibrium with the interior α solid solution. While the Ni-H phase diagram is not well established, it can be expected to be analogous to the Pd-H system. Under the high H fugacity during charging the

β hydride which forms on the surface may be expected to have a high H/Ni ratio at the surface with the H concentration decreasing to a value consistent with the β phase in equilibrium with the interior α solid solution. During the initial aging, the β phase will decrease its H/Ni ratio while the amount of the β remains the same. This leads to a decrease in the β lattice parameter (increase in $2\theta_{\{111\}^*}$) while the amounts of the β and α phases ($I_{\{111\}^*}$ and $I_{\{111\}}$) remain constantn (Fig. 3). Only after the β phase composition decreases to that in equilibrium with the α phase will the amount of the β phase decrease ($I_{\{111\}^*}$) while the H/Ni of the β phase remains at the equilibrium value. Throughout the aging period the lattice parameter of the α phase ($2\theta_{\{111\}}$) remains approximately constant as the H/Ni value for the α phase is very small.

The association of thee observations with adsorbed species has not previously been established. The usual behavior on aging in air at 298 K for specimens charged at 298 K at 500 A/m^2 for 20 min is shown by Fig. 4(a) where outgassing requires about 5×10^3 min for completion. In Figs. 4(b) and (c) show the behavior on outgassing after rinsing adsorbed species from the surface with flowing water for 15 minutes (solid points) after aging in air for 10 min (Curve b) and 2.5 min (Curve C) in air (open points). In contrast to curve (a), water rinsed specimens show much faster hydride decomposition rates, and the hydride decomposition is completed after aging for about 102 min.

The relation between decomposition of β hydride and the surface chemistry was also investigated using SIMS and AES techniques. Figure 5 shows the depth profiles of mass 2, ^2H, and mass 75, ^{75}As, for cathodically charged HP-Ni before and after a water rinse. The deuterium depth profile of the specimen taken immediately after cathodic charging and without a water

rinse, Fig. 5(a), showed a high, constant deuterium concentration near the surface to a depth of about 1 micrometer corresponding to the surface hydride. After a rinse in H_2O and a short age of 30 min at 298 K (Fig. 5(b)) the hydride was no longer present again indicating an accelerated rate of hydride decomposition due to the water rinse . Since the deuterium depth profile of characteristic of a surface hydride was still observed in specimens aged for 10 h at 298 K without a water rinse, the disappearance of the hydride in Fig. 5(b) is clearly caused by the water rinse itself. The SIMS depth profiles of ^{75}As (Fig. 5) showed no significant differences before and after the water rinse. This can result from two factors; a) the insensitivity of the SIMS method to the surface chemistry and b) the formation of NiOH, having mass 75, on the nickel surface during sputtering. Detection of changes in surface chemistry caused by the water rinse was carried out by AES studies which have much greater surface sensitivities. Auger line profiles of HP-Ni which was hydrogen charged (500 A/m^2 for 20 min) and aged in air (298 K for 3 days) without (Fig. 6(a)) and after (Fig. 6(b)) a water rinse clearly showed that the water rinse removed As and Cu from the nickel surface. Auger depth profiles of the specimen aged without and after the water rinse are shown in Fig. 7 where the removal of As and Cu from the specimen surface by the water rinse (Fig. 7(b)) is clearly shown. The depth profiles also show that the adsorbed species were surface adsorbed rather than being incorporated into the bulk of the hydride.

Since the hydride decomposition rate is sensitive to surface chemistry it may be expected that both the hydriding rate and the hydride decomposition rate will depend on the alloy composition; particularly if surface segregation of the alloying element occurs. Figure 8 shows the decomposition behavior of nickel hydride in air at 298 K after cathodic charging of HP-Ni, Ni-C, and Ni-S

alloys at a current density of 500 A/m^2 for 20 min. The decomposition rate of the surface hydride in the Ni-S alloy is slower, while that in Ni-C alloy it is faster than in HP-Ni. The average thickness of the surface hydride layer is almost identical among these three type of nickel alloys, as measured by the $I_{\{111\}^*}$ and SIMS, and was about 1 micrometer in thickness. The Auger depth profiles of these alloys showed no significant difference in the surface concentration or distribution of As and Cu between HP-Ni, Ni-S and Ni-C alloys nor was any evidence of C or S segregation seen. In the absence of the adsorbed As (removed by a 15 min. water rinse) the hydride decomposition rate was increased and was essentially identical in all the alloys (Fig. 9).

IV. DISCUSSION

As previously discussed, the x-ray results can be accounted for by hydride formation at the surface of the specimen in equilibrium with the solid solution at the specimen interior. This conclusion is consistent with the SIMS measurements where the ratio of the ^{2}H concentration in the surface layer to the interior is about equal to the ratio H_β/H_α expected from the phase diagram. Further direct evidence for surface hydride formation is shown by the fracture surfaces shown in Fig. 10 which are of HP-Ni cathodically charged at 500 A/m^2 for 13 hrs at 298 K. The surface hydride is clearly shown and it has a thickness of about 9 micrometers. Since the formation of the surface hydride at the α - β interface is limited by hydrogen diffusion through the β phase, its growth rate is proportional to $t^{1/2}_{charging}$. The observed 9 micrometer thickness for 13 hours of cathodic charging is consistent with the 1.5 micrometers observed after 20 min charging (Fig. 5) and with a H diffusivity in the β hydride at 293 K of 4.3×10^{-16} m^{2}s^{-1}.

The rate of hydride formation, i.e. the thickness of the surface hydride, is controlled by the flux of hydrogen through the β phase and hence is directly proportional to the surface fugacity Ie the surface concentration of H in the β phase). The role of surface adsorbed As in increasing the surface hydrogen fugacity and hence the hydrogen ingress is well established (1-6). These effects appear to result from As causing inhibition of the hydrogen recombination reaction

$$H(ads) + H(ads) \rightarrow H_2(g)$$

at the surface of the specimen thereby increasing the reaction rate for

$$H(ads) \rightarrow H(soln).$$

This effect can result from various surface phenomena including the "blocking" of surface sites (i.e. the exclusion of H occupancy of surface sites adjacent to the adsorbed As atoms) and thus preventing adsorbed H form occupying a near neighbor site to another adsorbed H.

Site blocking by adsorbed solutes can be expected to affect the egress of H from solids in the same manner and has been shown to decrease the flux from the solid to the gas in a permeation experiment (12). The effect of any adsorbed species can extend to blocking multiple nearest neighbor surface sites (12) thus decreasing the probability of having adsorbed hydrogen occupy close neighbors sites as required for the formation of H_2 molecules. This is consistent with the present results which show that adsorbed As does in fact decrease the reaction rate for the reaction H(ads.) + H(ads.) → H_2(g). A significant blocking reaction due to adsorbed As is consistent with the formation of a stable hydride, AsH_3 which is a gaseous hydride at 298 K. In aqueous solutions the more stable form is the hydrated compound $AsH_3 \bullet 6H_2O$ which is crystalline at 298 K. Gaseous AsH_3 has an enthalpy of formation ΔH^o_{298} = 172 KJ/mole while the AsH_3 formation enthalpy in the

hydrated form is 96 KJ/mole; both are formed by endothermic reactions. Removal of the adsorbed As by a rinse in H_2O may occur by the formation of ortho-arsenic acid, $H_3AsO \bullet 1/2\ H_2O$ which is a relatively stable compound (H^o_{298} = -900 KJ/mole) having significant solubility in cold water.

In principal effects similar to those due to adsorbed As can be observed with other adsorbed species. Blocking effects due to several adsorbed species have been seen on the exit surface during gas permeation (12). Other highly adsorbed species, such as thiourea (H_4CN_2S) and CS_2 in the electrolytic solution have been shown to result in increased hydrogen fugacity during cathodic charging and may also be expected to have an effect on the outgassing rate. This latter effect has not been studied. The Auger Spectroscopy results (Figs. 6 and 7) show evidence of both As and Cu adsorption on the surface of the electrolytically charged Ni. The effect of adsorbed Cu was studied by the addition of 10^{-5} M Cu^{2+} ions to the electrolytic charging solution, with all other charging conditions being held constant. As shown in Fig. 11 the addition of Cu^{2+} had little effect on the β hydride decomposition rate. The presence of Cu^{2+} actually increased the decomposition rate slightly, possibly as a result of replacement of some of the As adsorbed on the surface of Ni.

The lack of the effect of adsorbed Cu on the reaction H(ads) + H(ads) $\rightarrow$ H_2(g) can result from a number of factors. Copper does not form a stable hydride in the solid and in the gaseous state, CuH has an endothermic formation enthalpy of 276 KJ/mole (compared to 172 KJ/mole for gaseous AsH_3). The weaker Cu-H bonding is consistent with a lesser blocking effect due to adsorbed Cu. A smaller blocking effect of Cu is also consistent with the gaseous copper hydride being the diatomic CuH in contrast to the stable tri-hydride AsH_3.

The effects of adsorbed species on cathodic charging are explicable on the basis of the above discussion. Strongly adsorbed species from the electrolyte are effective in blocking the hydrogen recombination reaction if they form stable hydrides. Adsorbed As, S, and C, form stable compounds with H and hence block hydrogen recombination sites thus decreasing the reaction constant for H(ads) + H(ads) $\rightarrow$ H2(g) and increasing the effective input hydrogen fugacity. In the case of As, adsorption is competitive with removal of the As from the surface by formation of soluble As compounds. During application of the cathodic polarization the adsorption process dominates (13) as there is a continuous source of As^{+3} ionsand the effect is to block surface sites for $H_2(g)$ formation while in the absence of the polarization voltage the dissolution of the As occurs allowing increased rates of $H_2(g)$ formation.

The importance of surface adsorbed species in these processes is shown by the results of Fig. 9 where it was shown that HP-Ni, Ni-S, and Ni-C all exhibited similar β hydride decomposition rates after the adsorbed as was removed. In contrast, the hydride decomposition rates differ significantly between the alloys in the presence of adsorbed As (Fig. 8). These effects may reflect increased As adsorption by S in solid solution and the decreased adsorption by C in solid solution consistent with the small variations in the hydride thicknesses indicated by the $I_{\{111\}^*}$ (Fig. 8) after equivalent cathodic charging. These differences may result from formation of As complexes with C and S at the surfaces of the alloys.

V. CONCLUSIONS

1) The decomposition of β hydride formed on the surface of Ni by cathodic charging was studied as a function of the surface chemistry of the Ni. In

high purity Ni the decomposition of the β hydride was much slower than its rate of formation in the presence of surface adsorbed As. The decomposition rate was greatly increased when the adsorbed As was removed.

2) Auger electron spectroscopy indicated that during cathodic charging As was adsorbed on the surface and that the As remained on the surface during hydride decomposition. The surface adsorbed As can be removed by a 15 min. H_2O rinse.
3) The effect of adsorbed As on increasing the H fugacity during charging is closely related to the effect of As on decreasing the rate of β hydride decomposition.
4) It is proposed that adsorbed As has the effect of blocking the H occupancy of close neighbor surface sites thereby making recombination of adsorbed H to form H_2 (gas) less likely. As a result, the H charging fugacity is increased and the loss of H from the hydride (by H_2 formation) is decreased.
5) Copper was adsorbed on the surface of Ni during cathodic charging as was As. Studies of the hydride decomposition rates after hydride formation in solutions to which Cu^+ ions were specifically added showed that adsorbed Cu had no effect on the hydride decomposition rate.
6) In the presence of adsorbed As the H fugacity is increased by S and decreased by C in solid solution in the nickel. In the absence of adsorbed As the two alloys had the same hydride decomposition rates as high purity Ni.

Table 1. Chemical Compositions of Alloys (at.ppm)

	C	O	N	S
HP-Ni	19	11	<4	
Ni-C	4950	33	4	
Ni-S	21	17	4	150

REFERENCES

1. D. Alexeen and M. Polukarov, *Z Elektrochem.* **32**, 248 (1926).
2. J. McBreen and M.A. Genshaw, *Proc. of Conference on Fundamental Aspects of SCC* (Ed. by R.W. Staehle et al.), Ohio State Univ., p. 51 NACE, Houston (1969).
3. J.F. Newman and L.L. Shreis, *Corrosion Sci.* **9**, 631 (1969).
4. T. Zkroczymaki, Z. Szklarska - Smialomska, and M. Smialomski, *Werkat. Korros.* **26**, 617 (1975).
5. R. D. McCright and R. W. Staehle, *J. Electrochem. Soc.* **121**, 609 (1974).
6. H. Hagi and N. Ohtani, *Trans. JIM* **27** (4), 270 (1986).
7. M. Smialowski, *Proc. of Conf. on Stress Corrosion Cracking and Hydrogen Embrittlement of Iron Base Alloys* (Ed. by R. W. Staehle, J. Hachmann, R. D. McCright and J. E. Slater), p. 405, NACE, Houston (1977).
8. J. Pielaszek, *Bull. Acad. Polon. Sci. Ser. Sci. Chim.* **20**, 611 (1972).
9. H. K. Birnbaum, H. Fukushima, and J. Baker *Advanced Techniques for the Characterization of Hydrogen in Metals* (Ed. by N. Fiore and B. Berkowitz) p. AIME, Warrendale, PA (1982).
10. A. Janko, *Bull.. Acad. Polon. Sci. Ser. Sci. Chim.*, **8**, 131 (1960).
11. B. Baronowski and M. Smialowski, *Int. J. Phys. Chem. Solids* **12**, 206 (1959).
12. R. Sherman and H. K. Birnbaum, *J. of Less Common Metals* **105**, 339 (1985).
13. A. Kimura and H.K. Birnbaum, *Acta Metall.* **35**, 1077 (1987).

ACKNOWLEDGEMENT

This work was supported by the Office of Naval Research through grant number N00014-83-K-0468. The authors would like to acknowledge the use of and assistance from the Center for the Microanalysis of Materials at the Materials Research Laboratory.

FIGURE CAPTIONS

Fig. 1 X-ray diffraction patterns of HP-Ni. (a) before hydrogen charging. (b) immediately after charging (i_c = 500 A/m^{-2}, 20 min, 293 K). (c) hydrogen charged and aged in air at 298 K for 43 h.

Fig. 2. Variation of the peak height of the {111}* nickel hydride reflection with aging in air at 298 K.

Fig. 3. Effect of aging ain air t 298 K on the peak heights and position of the {111}* nickel hydride reflection, $I_{\{111\}^*}$, and its position, $2\theta_{\{111\}^*}$, compared to the nickel {111} reflection position and position, $I_{\{111\}}$ and $2\theta_{\{111\}}$. Hydrogen was charged at i_c = 500 A/m^2 for 20 min at 293 K.

Fig. 4. Effect of a water rinse on the hydride decomposition rate. After hydrogen charging (i_c = 500 A/m^2, 20 min, 293 K), specimens were (a) aged at 298 K in air without a water rinse. (b) aged 10 min at 298 K in air then water rinsed for 15 min at 293 K followed by aging in air at 298 K. (c) aged 2.5 min at 298 K in air then water rinsed for 15 min at 293 K followed by aging in air at 298 K.

Fig. 5. The SIMS depth profiling of masses 2, 12, 16, 58 and 75 (^2H, ^{12}C, ^{16}O, ^{58}Ni and ^{75}As (or $NiOH^-$)) of hydrogen charged HP-Ni (i_c = 500 A/m^2, 20 min, 293 K). (a) immediately after charging. (b) after a water rinse for 15 min at 293 K and aging in air at 298 K 30 min. The measurements were made at a specimen temperature below 200 K. The data are not normalized.

Fig. 6. AES spectra of the surface of HP-Ni charged with hydrogen (i_c = 500 A/m^2, 20 min, 293 K) and aged in air at 298 K for 3 days. (a) before 15 minute water rinse (b) after water rinse.

Fig. 7. AES depth profiling curves of As, Cu, O and C at the surface of hydrogen charged (i_c = 500 A/m^2 for 20 min at 293 K) and aged (3 days at 298 K) HP-Ni. (a) before a 15 minute water rinse. (b) after the water rinse.

Fig. 8. The difference of the hydride decomposition behavior at 298 K among HP-Ni (O), Ni-C (□) and Ni-S (Δ) after hydrogen charging (i_c = 500 A/m^2 for 20 min at 293 K).

Fig. 9. Same as Fig. 8 except for a water rinse of 15 min at 293 K after 2-5 min aging at 298 K in air.

Fig. 10. Fracture surfaces of HP-Ni electrolytically charged at i_c = 500 A/m^2 for 13 hrs and at 298 K.

Fig. 11. Effect of the addition of 10^{-5} M Cu^{2+} into the electrolyte on the hydride decomposition behavior. Specimens were charged with hydrogen at a current density of 500 A/m^2 for 20 min at 293 K and aged at 298 K.

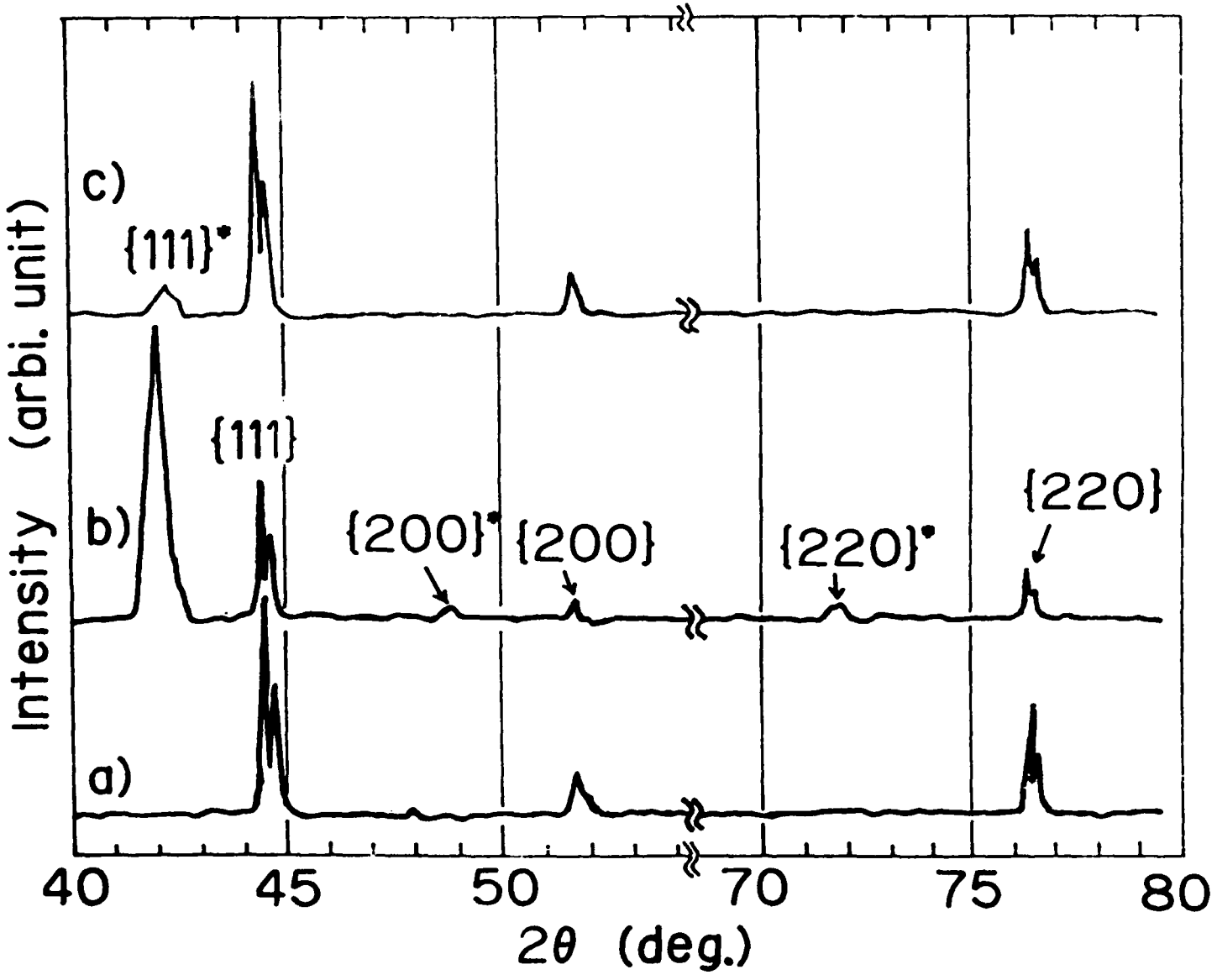
c)
{111}*
b)
{111}
{200}*
{200}
{220}*
{220}
a)
Intensity (arbi. unit)
40
45
50
70
75
80
2θ (deg.)

Fig. 1

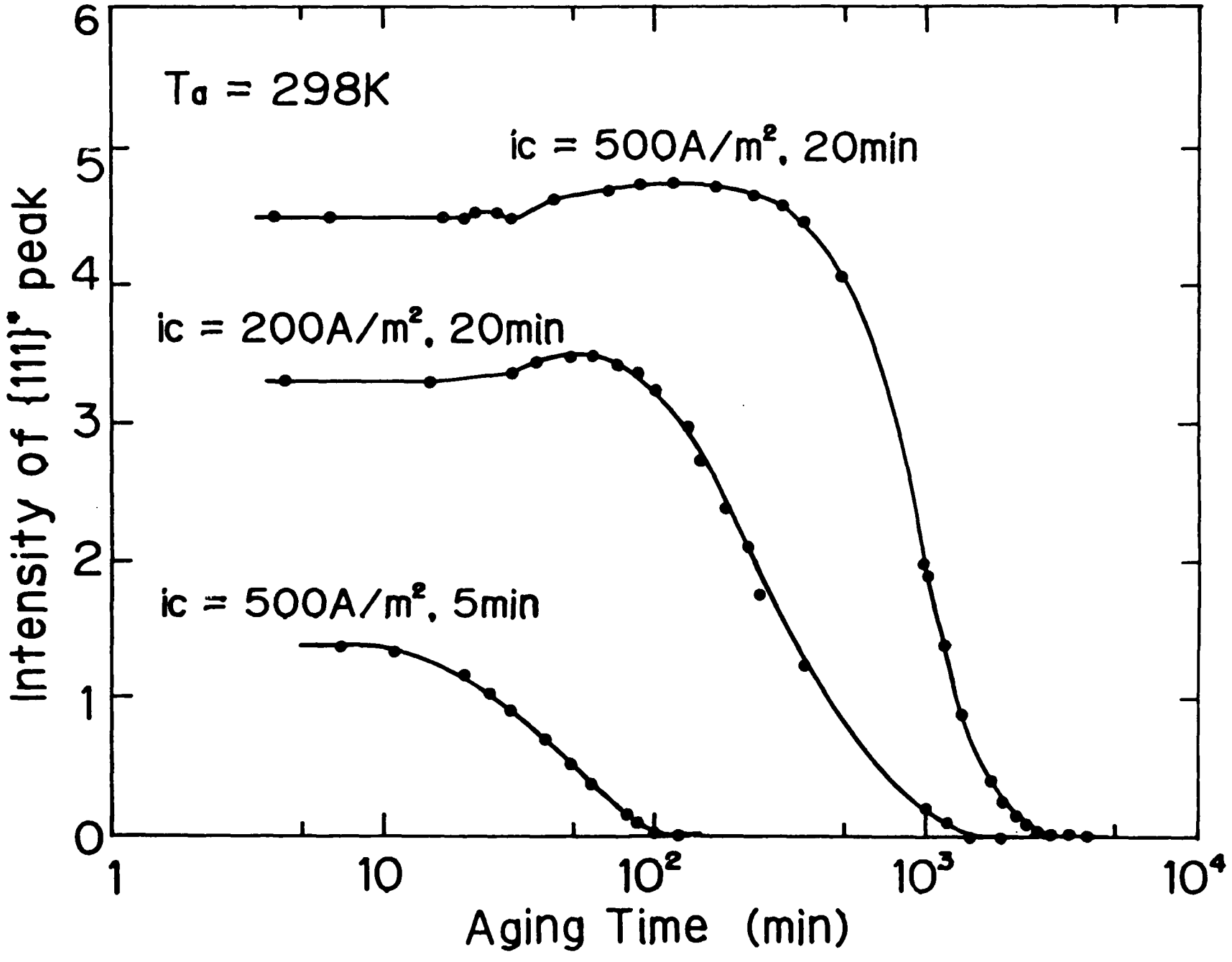
Ta = 298K
ic = 500A/m², 20min
ic = 200A/m², 20min
ic = 500A/m², 5min
Intensity of {111}* peak
Aging Time (min)
0
1
2
3
4
5
6
1
10
10²
10³
10⁴

Fig 2

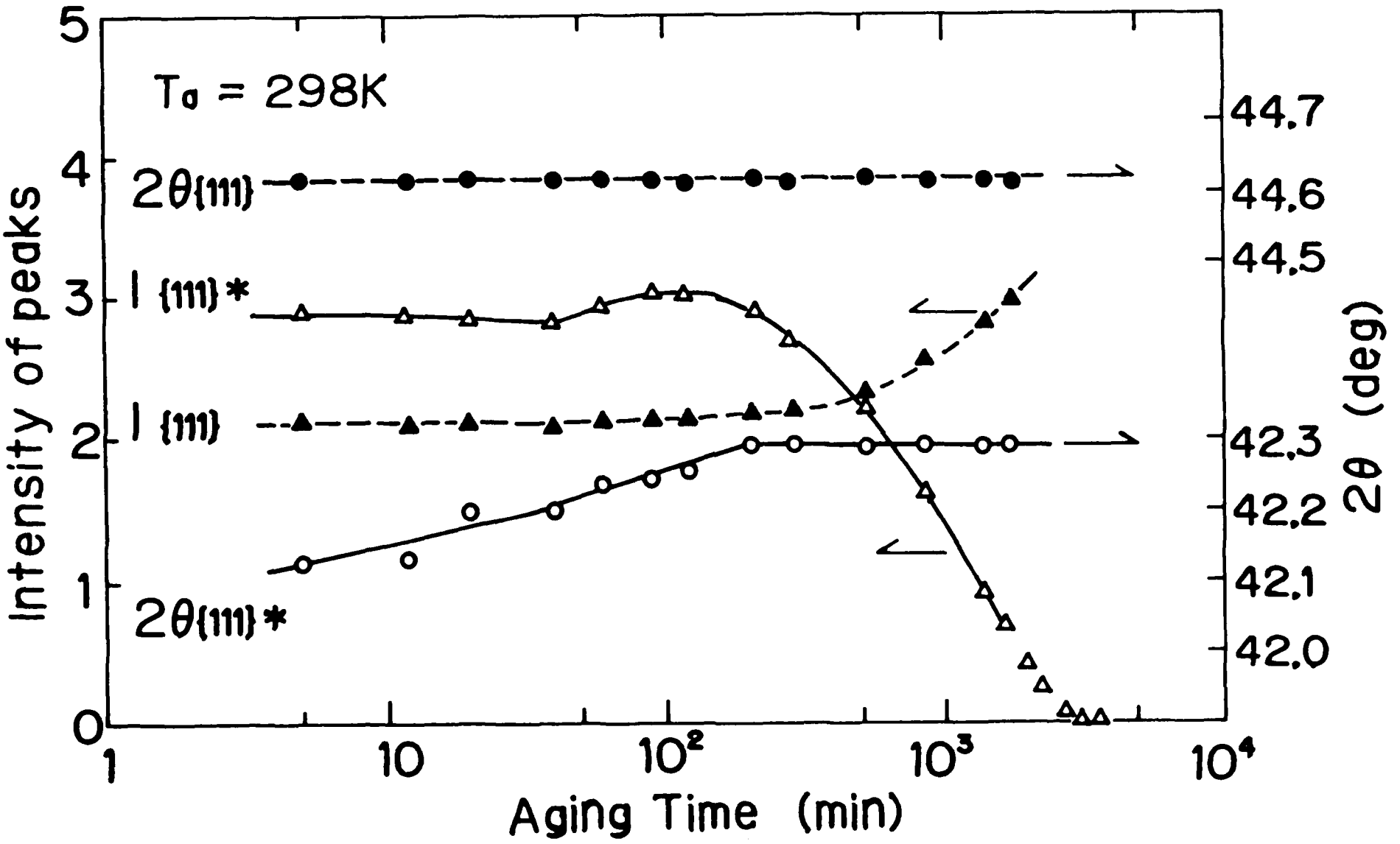
Ta = 298K
2θ{111}
I {111}*
I {111}
2θ{111}*
Intensity of peaks
2θ (deg)
Aging Time (min)
0
1
2
3
4
5
1
10
10²
10³
10⁴
44.7
44.6
44.5
42.3
42.2
42.1
42.0

Fig. 3

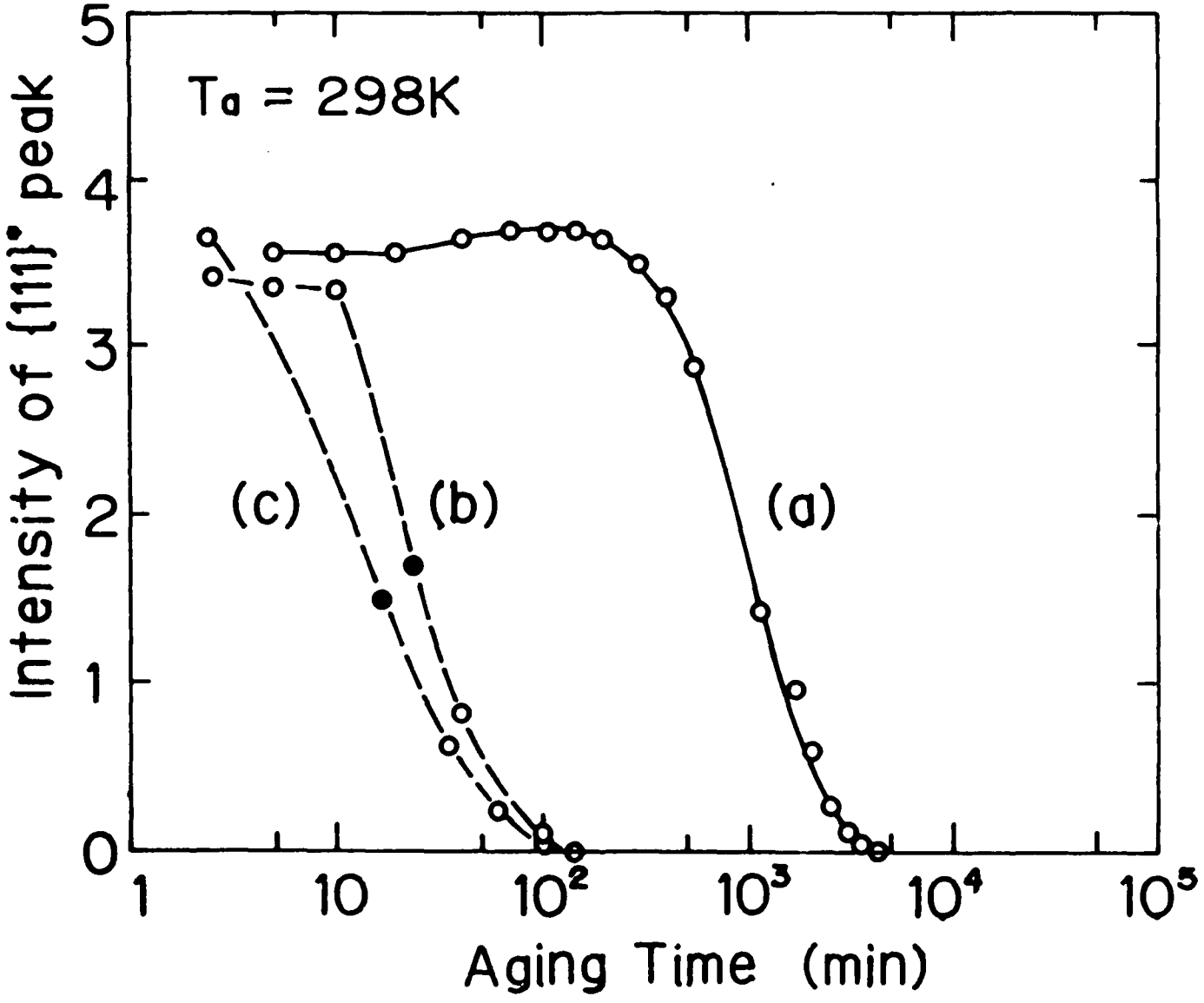
Ta = 298K
Intensity of {111}* peak
Aging Time (min)
(a)
(b)
(c)
0
1
2
3
4
5
1
10
10²
10³
10⁴
10⁵

Fig. 4

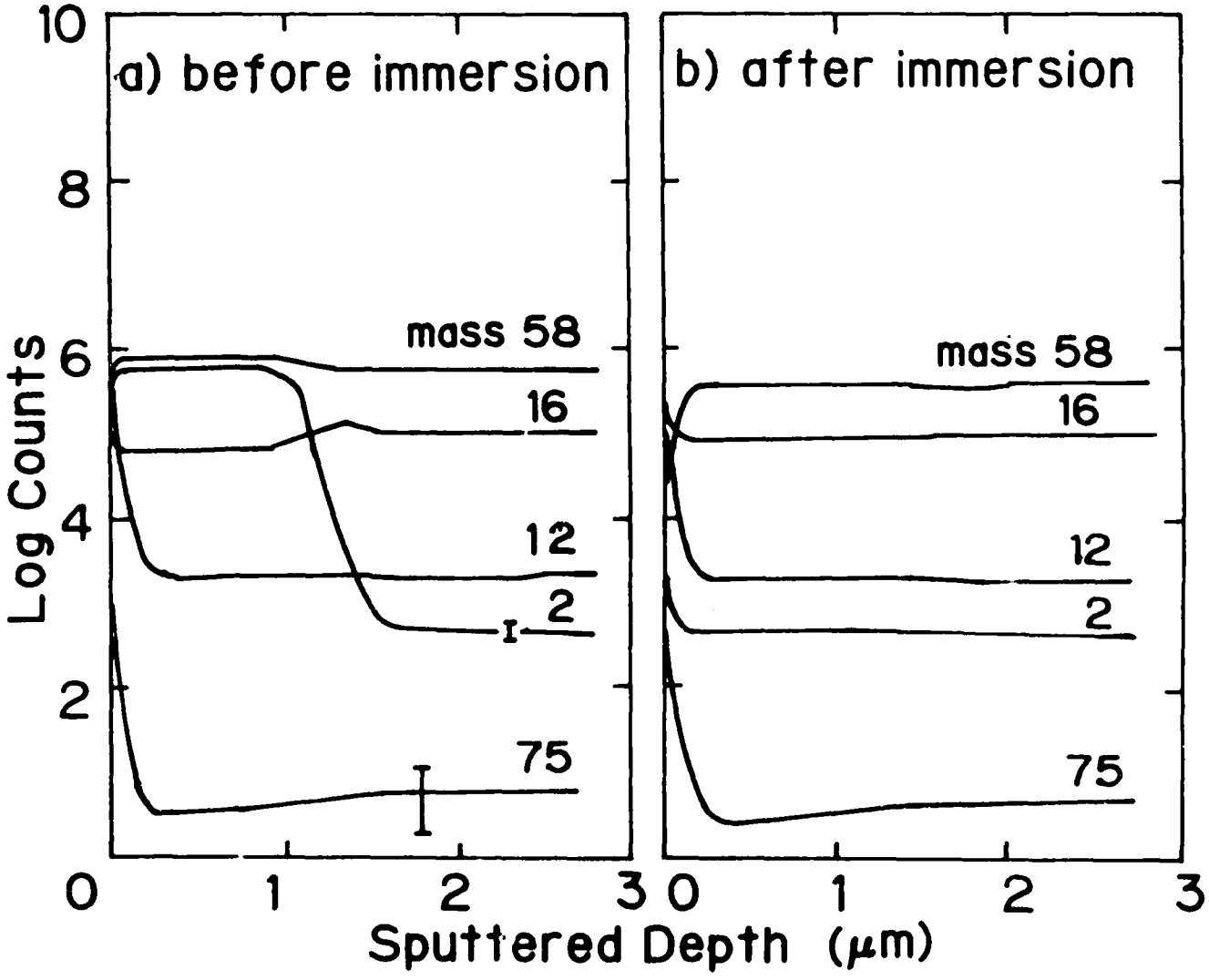
a) before immersion
b) after immersion
mass 58
16
12
2
75
Log Counts
10
8
6
4
2
0
1
2
3
Sputtered Depth (μm)

Fig 5

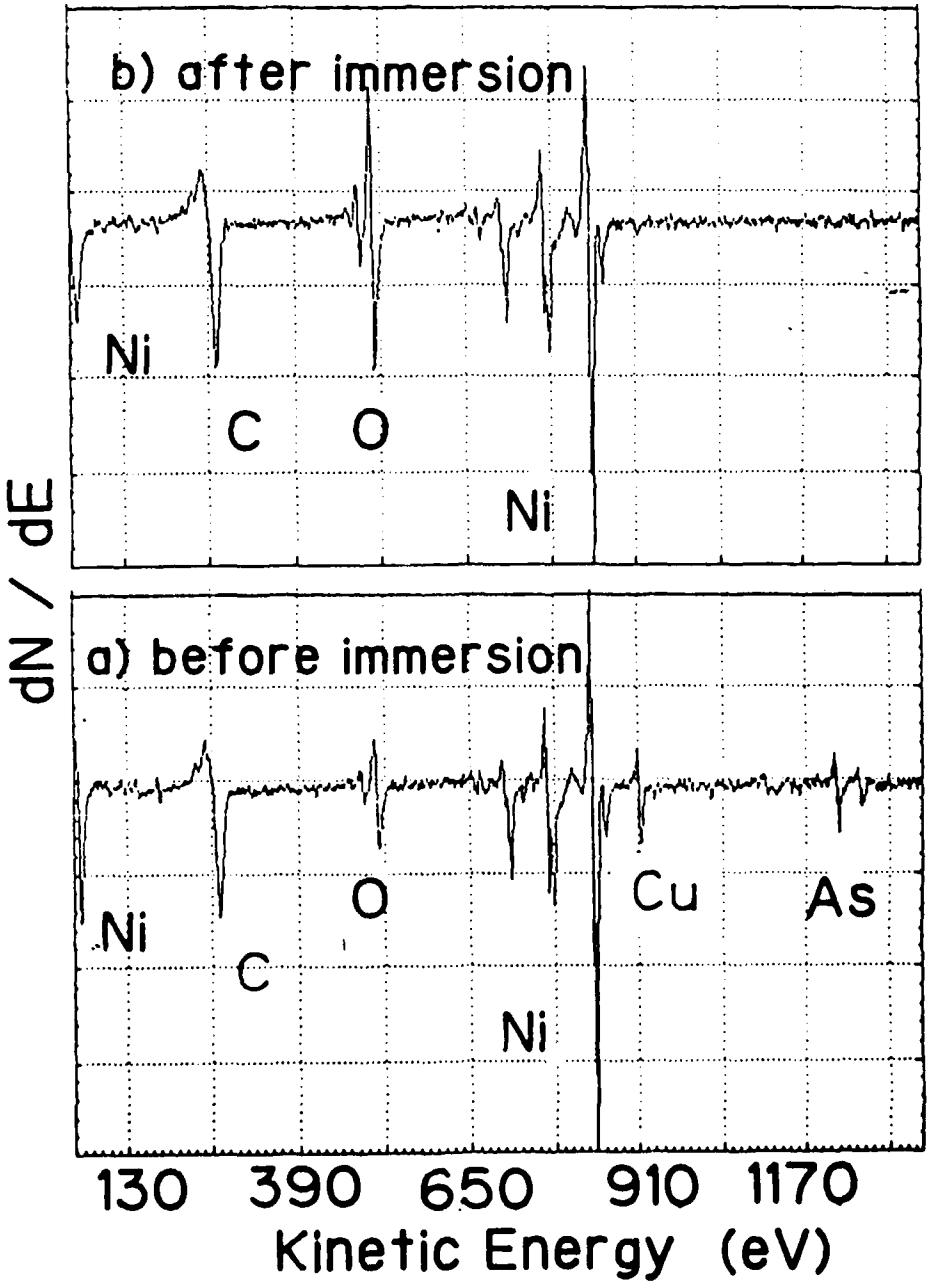
b) after immersion
Ni
C
O
Ni
a) before immersion
Ni
C
O
Ni
Cu
As
dN / dE
130
390
650
910
1170
Kinetic Energy (eV)

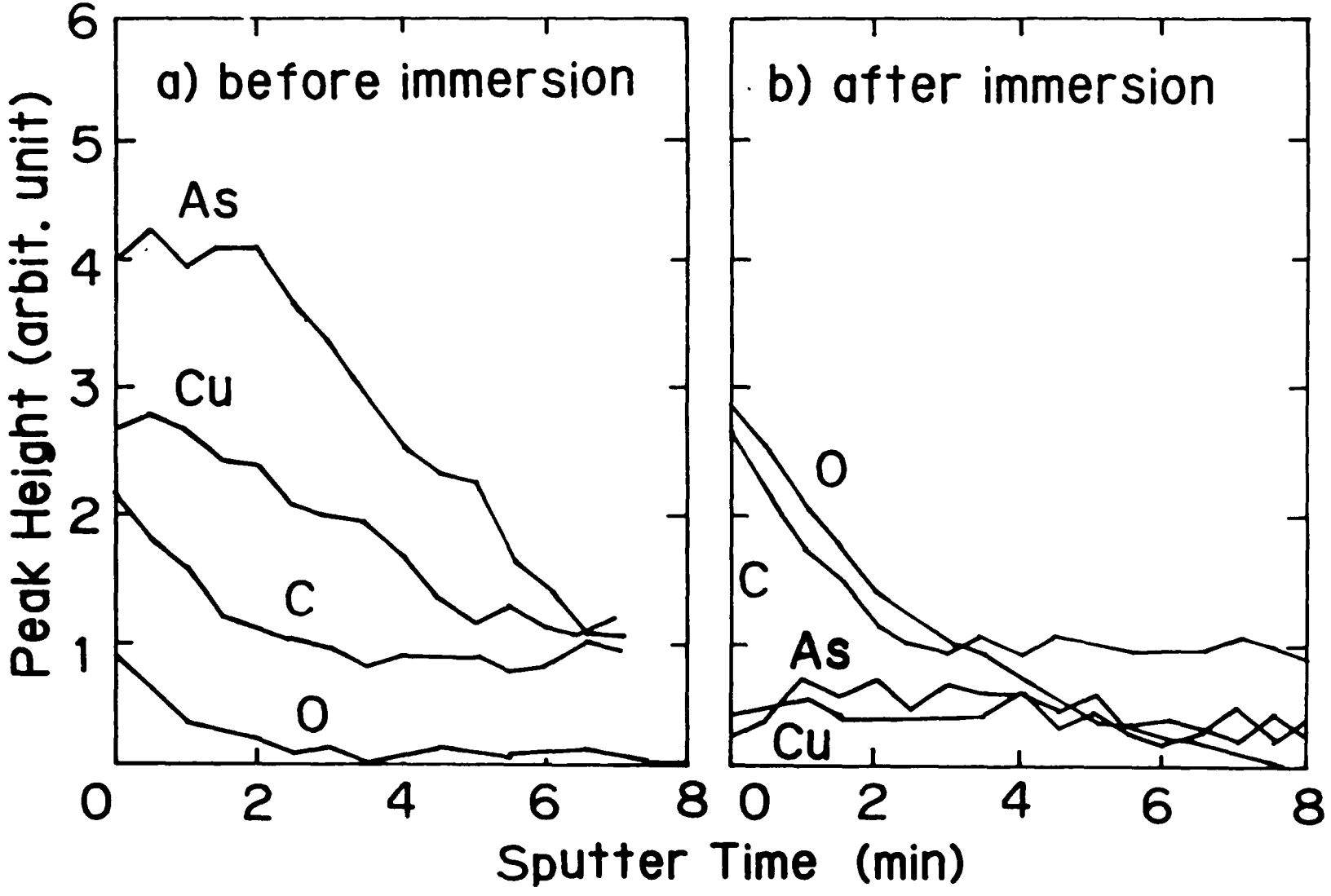
a) before immersion
b) after immersion
As
Cu
C
O
O
C
As
Cu
Peak Height (arbit. unit)
Sputter Time (min)
0
1
2
3
4
5
6
0
2
4
6
8
0
2
4
6
8

Fig. 7

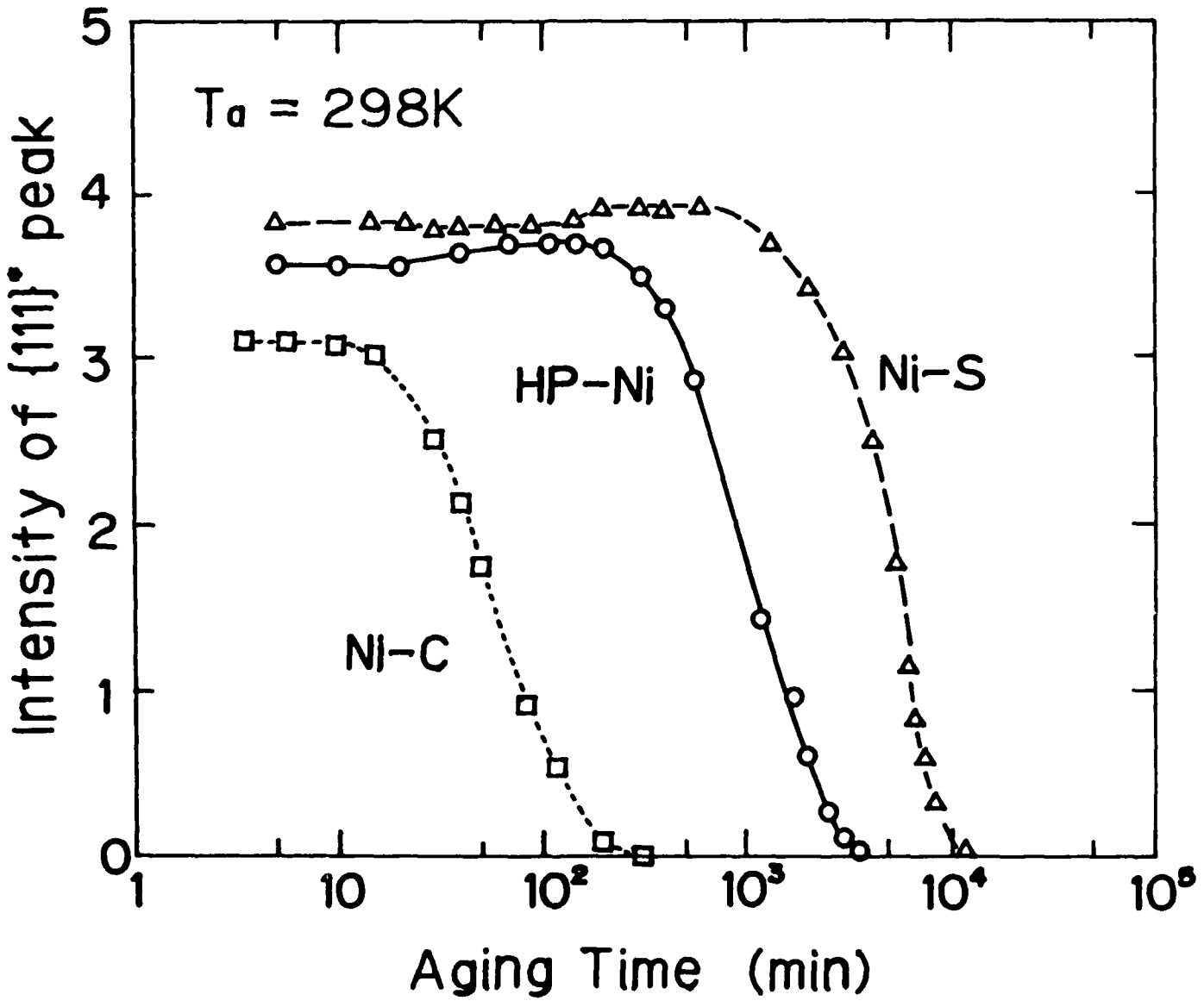
Ta = 298K
HP-Ni
Ni-S
Ni-C
Intensity of {111}* peak
Aging Time (min)
0
1
2
3
4
5
1
10
10²
10³
10⁴
10⁵

Fig. 8

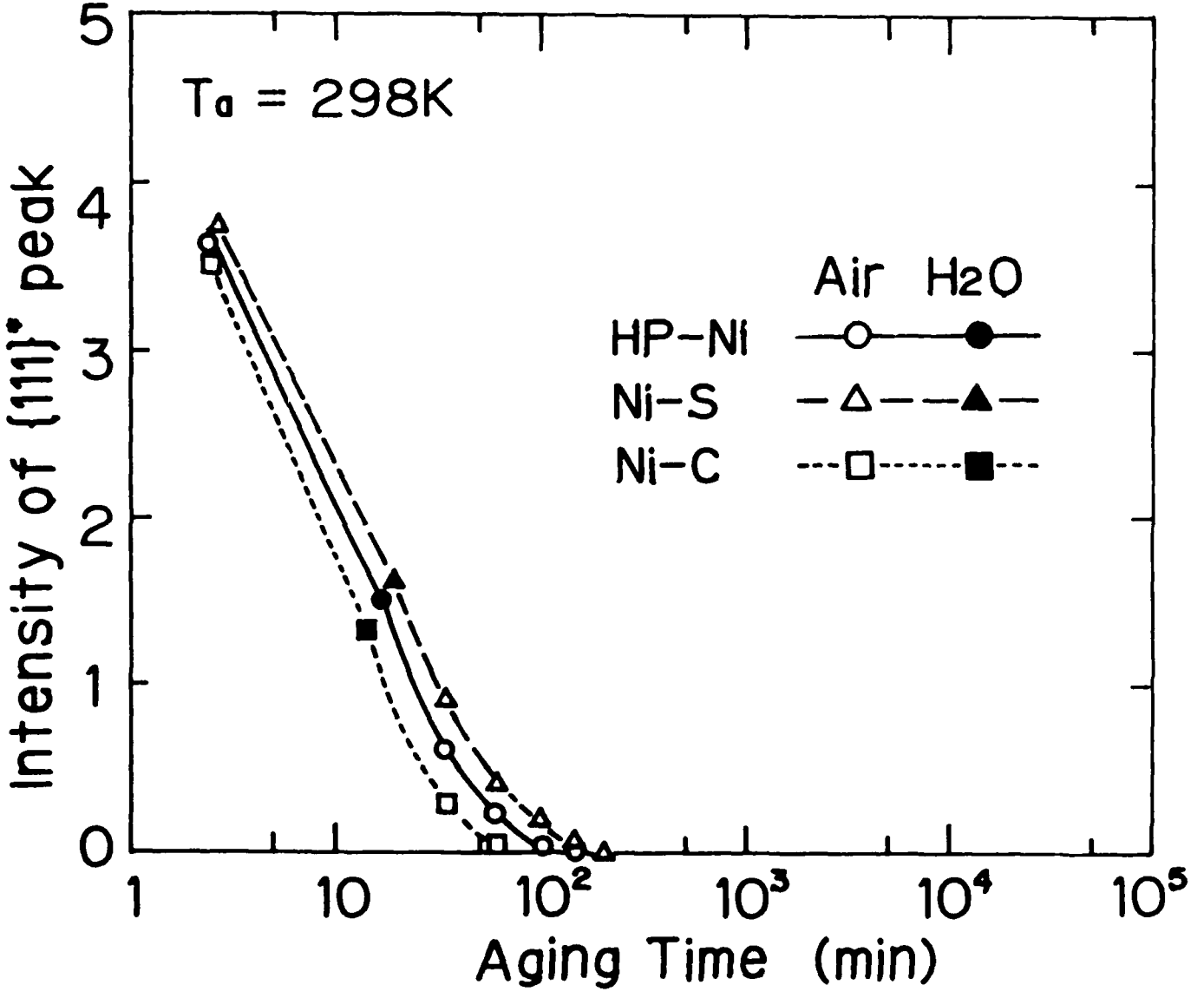
T_a = 298K
Intensity of {111}° peak
Aging Time (min)
Air H2O
HP-Ni
Ni-S
Ni-C
0
1
2
3
4
5
1
10
10^2
10^3
10^4
10^5

Fig. 9

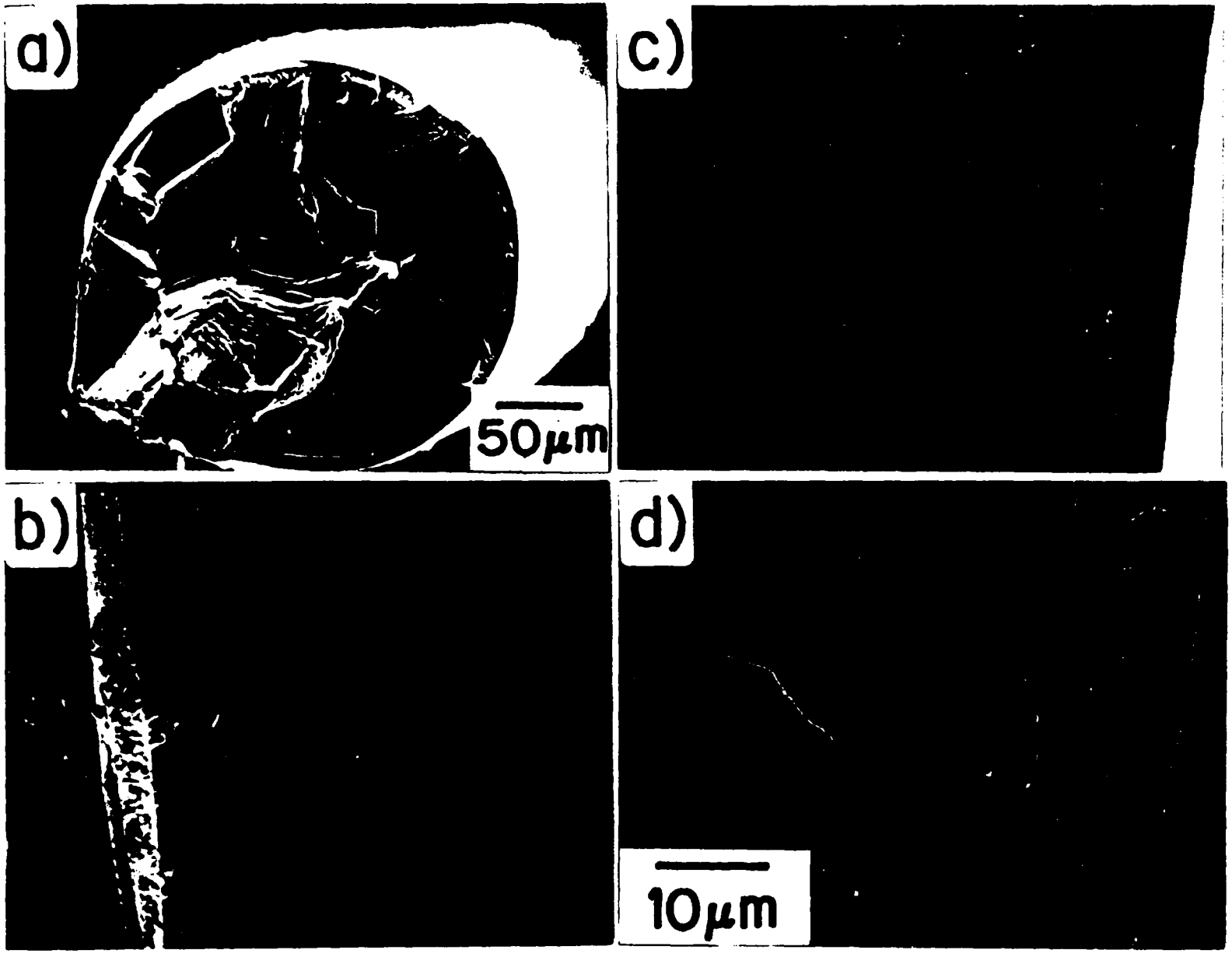

Fig. 10

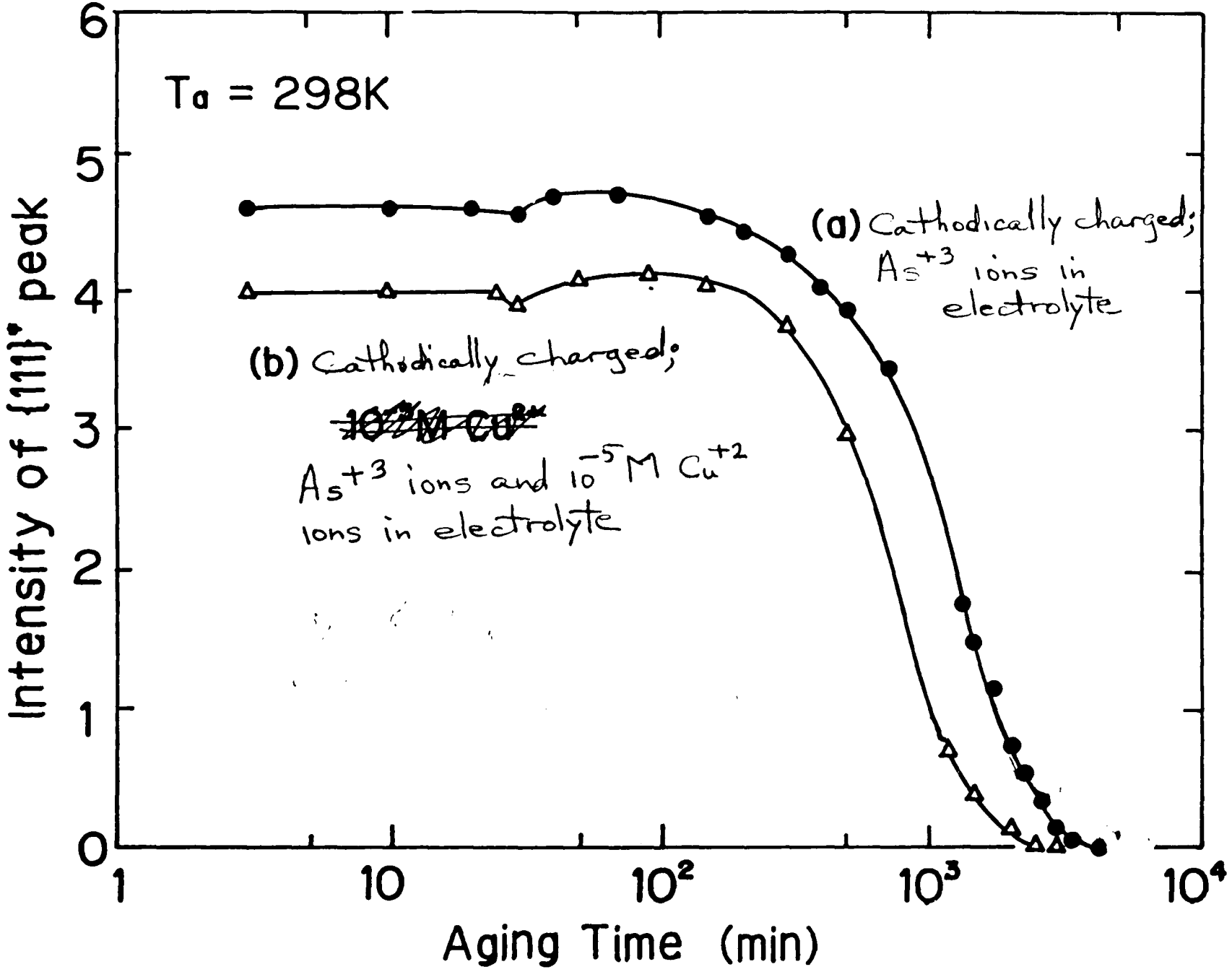
Ta = 298K
(a) Cathodically charged; As^{+3} ions in electrolyte
(b) Cathodically charged; As^{+3} ions and 10^{-5} M Cu^{+2} ions in electrolyte
Intensity of {111}* peak
Aging Time (min)
0
1
2
3
4
5
6
1
10
10^2
10^3
10^4

Fig. 11